Temperature-controlled optical activity and negative refractive index

Meng Liu, Eric Plum, Hua Li, Shaoxian Li, Quan Xu, Xueqian Zhang, Caihong Zhang, Chongwen Zou, Biaobing Jin, Jiaguang Han*, and Weili Zhang**

Dr. M. Liu, Dr. S.-X. Li, Dr. Q. Xu, Dr. X.-Q. Zhang, Prof. J.-G. Han
Center for Terahertz Waves and College of Precision Instrument and Optoelectronics Engineering, Tianjin University, Tianjin 300072, China
E-mail: jiaghan@tju.edu.cn

Dr. E. Plum
Centre for Photonic Metamaterials & Optoelectronics Research Centre, Zepler Institute, University of Southampton, Southampton, SO17 1BJ, UK.
E-mail: erp@orc.soton.ac.uk

H. Li, Prof. C.-H. Zhang, Prof. B.-B Jin,
Research Institute of Superconductor Electronics (RISE), School of Electronic Science and Engineering Nanjing University Nanjing 210093, P. R. China

Prof. W.-L. Zhang
School of Electrical and Computer Engineering, Oklahoma State University, Stillwater, Oklahoma 74078, USA
E-mail: weili.zhang@okstate.edu

Prof. C.-W. Zou
National Synchrotron Radiation Laboratory, University of Science & Technology of China Hefei 230029, P. R. China

Dr. M. Liu
College of Electronic and Information Engineering, Shandong University of Science and Technology, Qingdao 266590, P. R. China

Keywords: chirality, optical activity, negative refractive index, phase transition, metamaterial, active control

Chiral media exhibit optical activity, which manifests itself as differential retardation and attenuation of circularly polarized electromagnetic waves of opposite handedness. This effect can be described by different refractive indices for left- and right-handed waves and yields a

negative index in extreme cases. Here we demonstrate active control of chirality, optical activity and refractive index. These phenomena are observed in a terahertz (THz) metamaterial based on three-dimensionally (3D) chiral metallic resonators and achiral vanadium dioxide inclusions. The chiral structure exhibits pronounced optical activity and a negative refractive index at room temperature when vanadium dioxide is in its insulating phase. Upon heating, the insulator-to-metal phase transition of vanadium dioxide effectively renders the structure achiral, resulting in absence of optical activity and a positive refractive index. The origin of the structure's chiral response is traced to magnetic coupling between front and back of the structure, while the temperature-controlled chiral-to-achiral transition is found to correspond to a transition from magnetic to electric dipole excitations. The use of a fourfold rotationally symmetric design avoids linear birefringence and dichroism, allowing such a structure to operate as tunable polarization rotator, adjustable linear polarization converter and switchable circular polarizer.

1. Introduction

Over two centuries ago, François Arago discovered that quartz possesses the ability to rotate the polarization state of light.[1] Within a few decades, Louis Pasteur linked this effect of optical activity to chirality.[2] Optical activity corresponds to different refractive indices for left- and right-handed circularly polarized electromagnetic waves, resulting in polarization rotation (circular birefringence) and preferential absorption of one circular polarization (circular dichroism). Since then, it has been discovered that optical activity can be influenced by temperature,[3,4] magnetic field,[5] electric field[6,7] and light intensity.[8] However, optical activity is weak in natural materials, requiring interaction lengths that are large in comparison

to the wavelength to accumulate significant polarization changes. This is especially true at THz frequencies due to the large mismatch of THz wavelengths (hundreds of micrometers) and characteristic dimensions of crystal lattices and molecules (about a nanometer). Changes of optical activity due to temperature, fields or light intensity can reach the same order of magnitude as optical activity when phase transitions are involved, but typically they are orders of magnitude weaker, i.e. negligible. Much larger optical activity can be engineered in metamaterials as the characteristic dimensions of such artificial materials can be chosen to be comparable to the wavelength of the radiation of interest.[9-14] In some cases, circular birefringence has been sufficiently large to achieve a negative refractive index for one circular polarization or the other.[15,16] Electromechanically reconfigurable metamaterials have enabled substantial electric control over optical activity,[17-21] while phase transitions in THz metamaterials have enabled control over the related phenomena of asymmetric transmission[22] and chiral mirrors.[23]

Here we demonstrate temperature-controlled chirality, optical activity and index of refraction. Switching between effectively chiral and achiral structures is achieved by exploiting the insulator-to-metal phase transition of vanadium dioxide in a THz metamaterial. At room temperature, the metamaterial is an array of mutually twisted metallic split rings in parallel planes, exhibiting large circular birefringence, circular dichroism and a negative index of refraction. Upon heating above the phase transition temperature, vanadium dioxide gradually short circuits the gaps of the rings, resulting in an effectively achiral structure with negligible optical activity and positive refractive index. In its chiral state, optical activity is associated with magnetic resonant modes and magnetic coupling of the split rings, while in its achiral

state, the metamaterial exhibits an electric dipole response. The overall structure has fourfold rotational symmetry, which avoids linear birefringence and dichroism, allowing such metamaterials to operate as temperature-controlled polarization rotator, linear polarization converter and circular polarizer.

2. Design and characterization

The temperature-controlled 3D-chiral metamaterial is shown by **Figure 1**. It is based on pairs of metallic split ring resonators (SRRs) separated by a dielectric spacer. Looking along +*z*, 3D chirality arises from a 90° clockwise rotation of the back SRRs relative to the corresponding front SRRs (Figure 1a). Four such split ring pairs are combined to form a four-fold rotationally symmetric unit cell that ensures an isotropic response to normally incident radiation due to absence of in-plane preferred directions (Figure 1b). Temperature-control of the metamaterial is enabled by placing each SRR pair in between a pair of matching continuous vanadium dioxide (VO_2) rings, such that the heating-induced dielectric-to-metal phase transition of VO_2 short-circuits the gap of each SRR. This phase transition of VO_2 occurs at a characteristic temperature of 65 ~ 68 °C and is accompanied by a drastic change in conductivity exceeding four orders of magnitude.[24-26] Thus, heating transforms the 3D-chiral metamaterial into an effectively achiral structure.

In order to fabricate the structure, identical arrays of 150-nm-thick VO_2 square rings were patterned on two sapphire substrates by optical lithography and plasma etching (CF_4/O_2). In a second lithography step, a gold SSR of 200 nm thickness was formed on top of each VO_2 ring by gold deposition, patterning and lift-off (Figure 1c). Then the metamaterial was assembled

by stacking the two structurally identical components with a mutual rotation of 90° and spaced by a lossy polyimide slab of 33 μm thickness. The metamaterial has a size of 1 cm × 1 cm and a square period of 135 μm.

The spectral response of this metamaterial was optimized by parametric analysis using CST Microwave Studio™. Taking advantage of structure's periodicity, we modelled a single unit cell with periodic boundary conditions in the lateral directions. Open boundary condition were applied in the propagation direction. The different materials were described by a conductivity of 3.56×10^7 S/m for gold, a dielectric constant of 9.67 for sapphire and a dielectric constant of 2.93 with loss tangent delta of 0.044 for polyimide. VO_2 was modelled with conductivities ranging from 10 S/m[24] to 2.6×10^5 S/m[24,27,28], corresponding to its insulating and metallic phases, respectively.

The chiral metamaterial was characterized by THz time-domain spectroscopy (THz-TDS). The transmission coefficients of the fabricated metamaterial were measured for the normally incident THz waves (along $+z$) at temperatures ranging from 23 to 102 °C. Within the THz-TDS setup, a mode-locked laser centered at 780 nm wavelength with 35 fs pulse duration and 78 MHz repetition rate is split into equal intensity beams (10 mW). Each beam is then focused on the surface of a different photoconductive antenna. One section is used to generate the THz transient by excitation of a biased photoconductive antenna, while the other section acts as a gate in a photoconductive receiver to detect the THz pulse coherently. The temporal shape of the THz transient is recorded by gradually changing the relative delay between THz transient and gate pulse while monitoring the current induced in the external circuitry by the THz field. The signal to noise ratio of the THz-TDS system exceeds 5000:1 in the experimental frequency

range of 0.4–1.0 THz. Fabricated samples are fixed to an electrically controlled heater which has an aperture at the center. Transmission measurements are performed in a drying chamber and four polarizers are employed to select and transform THz polarizations since only horizontally polarized THz waves are efficiently radiated and detected in this THz-TDS system. All presented THz transmission measurements were normalized to spectra of a sample without gold and without VO_2 structures. Transmission characteristics for circularly polarized waves were determined by transformation from the linear polarization basis to the circular polarization basis as described in [22].

3. Results and discussion

The transmission characteristics of the metamaterial, as it transitions from its room temperature chiral state to its high temperature achiral state, were simulated and measured. The metamaterial's chiral state, which has insulating SRR gaps, is modelled with a VO_2 conductivity of 10 S/m and measured at room temperature. The phase transition is studied by increasing the metamaterial temperature and simulated by increasing the conductivity of VO_2, which effectively eliminates the chirality of the structure by gradually short circuiting the SRR gaps. The effectively achiral state is measured at the maximum accessible temperature of 102 °C and modelled with a VO_2 conductivity of 2.6×10^5 S/m.

Figure 2 shows the metamaterial's temperature-dependent transmittance spectra for THz waves of left-handed circular polarization (LCP, shown left) and right-handed circular polarization (RCP, shown right) according to simulations (top) and measurements (bottom). Here we define RCP (+) as clockwise rotation of the electric field at a fixed position as seen

by an observer looking into the THz beam towards the source. $|T_{ij}|^2$ represents the *i*-polarized transmittance of the sample resulting from the *j*-polarized illumination. T_{ij} is the corresponding field transmission coefficient, relating transmitted and incident electric fields according to $E_i^{trans} = T_{ij}\, E_j^{inc}$. Circular polarization conversion cannot occur at normal incidence due to the structure's isotropic (four-fold rotationally symmetric) design, and indeed $|T_{+-}|^2$ and $|T_{-+}|^2$ are zero within numerical and experimental accuracy in all cases. It follows, that the structure can be described in terms of circularly polarized eigenstates. The metamaterial's co-polarized transmittance spectra are strongly dependent on temperature (VO_2 conductivity). At room temperature (10 S/m), the spectral dependencies of $|T_{--}|^2$ and $|T_{++}|^2$ are different from each other, exhibiting a pronounced resonance just above and just below 0.65 THz, respectively. The difference between $|T_{--}|^2$ and $|T_{++}|^2$ reveals the presence of circular dichroism, i.e. chirality of the metamaterial response at room temperature. As the metamaterial is heated above the dielectric-to-metal phase transition of VO_2 to 102 °C (2.6×10^5 S/m), the resonances vanish and $|T_{--}|^2$ and $|T_{++}|^2$ become (almost) identical, which is consistent with the expected achiral metamaterial response at high temperatures. The observed behavior corresponds to a thermally switchable notch filter exhibiting different low-temperature stop bands for LCP and RCP, which are separated by 0.035 THz and 0.065 THz according to simulations and experiments, respectively.

Figure 3 illustrates the active thermal control over the metamaterial's chiral response in terms of the manifestations of optical activity: circular dichroism (differential transmittance of circularly polarized waves, $|T_{++}|^2 - |T_{--}|^2$) and circular birefringence (differential retardation of circularly polarized waves, $\angle T_{++} - \angle T_{--}$). When the metamaterial is in its chiral state, i.e. at

low temperatures (low VO_2 conductivity), strong circular dichroism and circular birefringence are associated with the resonance around 0.65 THz. As the structure is heated, its optical activity reduces gradually and dramatically in the 67 – 75 °C temperature range, i.e. around the dielectric-to-metal phase transition temperature of VO_2. At higher temperatures (i.e. at high VO_2 conductivity), the chiral response vanishes almost entirely, i.e. circular dichroism and birefringence become negligible. Thus, the metamaterial is a thermally tuneable optically active element. At selected frequencies and room temperature, the structure acts as circular polarizer, with an experimentally observed polarization contrast $|T_{-+}|^2 / |T_{++}|^2$ reaching up to 7.8. At the maximum of circular birefringence, which coincides with vanishing circular dichroism, the device acts as polarization rotator, with experimentally observed polarization rotation of up to 33.5° (half of the circular birefringence). Both functions, circular polarizer and polarization rotator, can be switched off by heating the device to a temperature well-above the dielectric-to-metal phase transition temperature of VO_2.

Active control of the metamaterial's optical activity also manifests in its transmission characteristics for linearly polarized THz waves, see **Figure 4**. Due to its four-fold rotational symmetry, the metamaterial properties are the same for normally incident waves of x, y or any other linear polarization. Therefore, the metamaterial can be characterized by transmission amplitudes for incident and transmitted waves with either parallel or orthogonal linear polarizations, $|T_{\parallel}|$ and $|T_{\perp}|$. (Indeed, $|T_{\parallel}|=|T_{xx}|=|T_{yy}|$ and $|T_{\perp}|=|T_{yx}|=|T_{xy}|$ within numerical and experimental accuracy.) At room temperature (low VO_2 conductivity), the metamaterial's resonance is associated with a minimum of co-polarized transmission $|T_{\parallel}|$ and a maximum of cross-polarized transmission $|T_{\perp}|$. The latter arises from substantial rotation of the transmitted

polarization state (circular birefringence), and in case of elliptical polarization of the transmitted wave also from circular dichroism. Upon heating, the metamaterial's resonant and chiral response weakens dramatically in the temperature window of 67 – 75 °C, resulting in negligible polarization changes at higher temperatures. Thus, the metamaterial allows active polarization control and can be used to convert a tuneable fraction of a linearly polarized incident THz wave to the orthogonal polarization state.

In order to reveal the microscopic origin of the metamaterial's chiral and achiral responses at low and high temperatures, we simulated the modes excited by *x*-polarized illumination at 0.65 THz, see **Figure 5**. The surface current oscillations are revealed by magnetic field perpendicular to the SRR planes, which arises from current oscillations within SRRs according to Ampère's Law. Our simulations reveal two types of current distributions, magnetic and electric dipole modes, **m** and **d** as shown in Figure 5.

The origin of the metamaterial's chiral response at low temperatures (10 S/m VO_2 conductivity) can be understood by considering how the magnetic dipole modes cause linear polarization conversion. Strong, resonant magnetic dipole modes are excited when the incident electric field is parallel to the middle of an SRR wire (e.g. SRRs 1^f and 2^b). They are looped **LC** charge oscillations on the SRR that correspond to a magnetic moment oscillating perpendicular to the SRR. This magnetic moment then excites a (somewhat weaker) magnetic mode of the corresponding 90°-rotated SRR in the other layer (e.g. SRRs 1^b and 2^f). The middle section of that 90°-rotated SRR wire then radiates THz radiation with 90°-rotated polarization, causing optical activity.

Short-circuiting of the SRR gaps at high temperatures (2.6×10^5 S/m VO_2 conductivity)

transforms the SRRs into continuous rings, which cannot support the magnetic mode. As a result, only electric dipoles consisting of pairs of weak, non-resonant, parallel charge oscillations can be excited in the structure. These electric dipoles, which are oriented parallel to the excitation field, can only reradiate the incident polarization state, causing an achiral response and transmission without polarization change.

Optical activity breaks the degeneracy of the refractive indices for circularly polarized waves of opposite handedness. The difference between the real parts of the refractive indices for LCP and RCP is proportional to circular birefringence, while the difference between the imaginary parts of the refractive indices is linked to circular dichroism. Therefore, metamaterials with strong circular birefringence can exhibit a negative refractive index for one circular polarization. Retrieval of the effective refractive indices[15,16,29-31] of the 3D-chiral metamaterial from our simulations reveals negative values around the metamaterial's 0.65 THz resonance when VO_2 is in the dielectric phase, see Supplementary **Figure S1**. Around the resonance, the refractive indices are strongly dependent on the conductivity of VO_2. For example, at a frequency of 0.63 THz the real part of the refractive index for RCP increases from -5.7 via zero to +3.1 while the refractive index for LCP reduces from +4.8 to +3.1 as VO_2 transitions from insulating to metallic, see **Figure 6a**. Similarly dramatic switching of the refractive index for LCP from strongly negative, via zero to positive occurs at a frequency of 0.66 THz, see **Figure 6b**. In all cases, the refractive indices for RCP and LCP converge as optical activity vanishes when the metamaterial is heated to its achiral high-temperature state. Thus, the dielectric-to-metal phase transition of vanadium dioxide enables dynamic control over the refractive indices for circularly polarized THz waves, where the real part can be tuned from negative via zero to

positive values.

Despite qualitative agreement, we note that resonances and associated chiral effects are generally weaker in our experiments than in our simulations. This may be due to fabrication inaccuracies and larger losses in the experimental structure. The magnitude of refractive index changes in our experiments can be estimated from the measured circular birefringence of up to 67° at 0.665 THz (Figure 3d). Considering the metamaterial thickness of 33.7 μm, this corresponds to a difference of 2.5 between the real parts of the refractive indices for LCP and RCP at room temperature, which vanishes when the metamaterial is heated. It follows that the temperature-controlled refractive index changes in our experiments exceed 1 refractive index unit.

While we observe very large chiral effects from just two layers of mutually twisted gold resonators, we note that even stronger effects may be expected from an increased number of layers of mutually twisted resonators.[15, 32] Furthermore, our metamaterial structure is quite sparse, with clusters of resonators separated by significant gaps. Therefore, a denser structure – with reduced or eliminated gaps between the resonant clusters – may be expected to yield enhanced chiral effects.

In comparison to electromechanical metamaterials,[17-21] control of chirality and its manifestations through a phase transition has the fundamental advantage that it does not require any moving parts. Absence of mechanical components simplifies the fabrication and can improve the structure's reliability and speed. While the response time of a mechanical structure is limited by its fundamental mechanical resonance, phase transitions can be very fast. Indeed, THz metamaterials with characteristic length scales of 100 μm or more have sub-MHz

mechanical resonances and will respond on milli- to microsecond timescales. In contrast, optical switching of VO_2 with picosecond optical pulses has been reported.[33]

4. Conclusion

We have demonstrated temperature-control of optical activity and index of refraction in a THz metamaterial. The structure exploits the dielectric-to-metal phase transition of vanadium dioxide to switch between chiral and effectively achiral resonator geometries. This allows its chiral properties, which are exceptionally strong at room temperature, to be tuned and even switched off by heating. We have observed thermal control over circular birefringence, circular dichroism, linear polarization conversion and refractive index. Indeed, our simulations indicate that the real parts of the refractive indices for circularly polarized waves can be controlled from negative via zero to positive values. The metamaterial's chiral response at low temperatures has been traced to magnetic dipole excitations, which couple between different layers of the 3D-chiral metamaterial. Its achiral response at high temperatures has been explained by electric dipole excitations. Chiral phase change metamaterials like the one presented here may find applications in active polarization control as tunable polarization rotators, switchable circular polarizers as well as tunable polarization-selective spectral filters.

Supporting Information

Supporting Information is available from the Wiley Online Library or from the author. The data from this paper are openly available from the University of Southampton ePrints research repository at https://doi.org/10.5258/SOTON/D1646, reference number [34].

Acknowledgements

This work was supported by the National Science Foundation of China (Grant Nos. 61935015, 61875150 and 62025504), the Tianjin Municipal Fund for Distinguished Young Scholars (18JCJQJC45600) and the UK's Engineering and Physical Sciences Research Council (grant EP/M009122/1).

Conflict of Interest

The authors declare no conflict of interest.

Author Contributions

M. Liu. conducted the experiments and simulations. M. Liu., H. Li, C.-H. Zhang, C.-W. Zou and B.-B. Jin fabricated the metamaterial structures. M. Liu, E. Plum, S.-X. Li., Q. Xu., X.-Q. Zhang, J.-G. Han and W.-L. Zhang interpreted the results. M. Liu and E. Plum wrote the manuscript. E. Plum, J.-G. Han and W.-L. Zhang supervised the project. E. Plum proposed the project.

References

[1] F. J. D. Arago, *Mémoires de la classe des sciences mathématiques et physiques de l'Institut Impérial de France, 1st part* **1811**, 93-134

[2] L. Pasteur, *Annales de chimie et de physique 3rd series*, **1850**, 28, 56-99

[3] C. W. Smith, D. G. Gisser, M. Young, and S. R. Powers, *Appl. Phys. Lett.* **1974**, 24, 453-454

[4] H. Goto and K. Akagi, *Angew. Chem.* **2005**, 117, 4396-4402

[5] M. Faraday, “Nov. 12, 1839 - June 26, 1847,” in Faraday’s Diary (George Bell and Sons, Ltd., 1933), Vol. 4. Faraday, Michael (1933). Faraday's Diary. Volume IV, Nov. 12, 1839 - June 26, 1847 (Thomas Martin ed.). London: George Bell and Sons, Ltd. ISBN 978-0-7503-0570-9.

[6] K. Aizu, *Phys. Rev.* **1964**, 133, A1584

[7] N. I. Zheludev, *Sov. Phys. Cryst.* **1965**, 9, 418-420

[8] S. A. Akhamanov, B. V. Zhdanov, N. I. Zheludev, N. I. Kovrigin, and V. I. K.uznetsov, *JETP Lett.* **1979**, 29, 264

[9] E. Plum, V. A. Fedotov, A. S. Schwanecke, N. I. Zheludev, and Y. Chen, *Appl. Phys. Lett.* **2007**, 90, 223113

[10] N. Liu, H. Liu, S. Zhu, and H. Giessen, *Nat. Photonic*s **2009**, 3, 157-162

[11] Y. Cui, L. Kang, S. Lan, S. Rodrigues, and W. Cai, *Nano Lett.* **2014**, 14, 1021-1025

[12] M. Esposito, V. Tasco, F. Todisco, M. Cuscuna, A. Benedetti, D. Sanvitto, and A. Passaseo, *Nat. Commun.* **2015**, 6, 6484

[13] M. Hentschel, M. Schaferling, X. Y. Duan, H. Giessen, and N. Liu, *Sci. Adv.* **2017**, 3

[14] I. Fernandez-Corbaton, C. Rockstuhl, P. Ziemke, P. Gumbsch, A. Albiez, R. Schwaiger, T. Frenzel, M. Kadic, and M. Wegener, *Adv. Mater.* **2019**, 31, e1807742

[15] E. Plum, J. Zhou, J. Dong, V. A. Fedotov, T. Koschny, C. M. Soukoulis, and N. I. Zheludev, *Phys. Rev. B* **2009**, 79

[16] S. Zhang, Y. S. Park, J. Li, X. Lu, W. Zhang, and X. Zhang, *Phys. Rev. Lett.* **2009**, 102, 023901.

[17] T. Kan, A. Isozaki, N. Kanda, N. Nemoto, K. Konishi, H. Takahashi, M. Kuwata-

Gonokami, K. Matsumoto, and I. Shimoyama, *Nat. Commun.* **2015**, 6, 8422

[18] T. Kan, A. Isozaki, N. Kanda, N. Nemoto, K. Konishi, M. Kuwata-Gonokami, K. Matsumoto, and I. Shimoyama, *Appl. Phys. Lett.* **2013**, 102, 221906.

[19] L. Cong, P. Pitchappa, N. Wang, and R. Singh, *Research (Wash D C)* **2019**, 7084251

[20] W. J. Choi, G. Cheng, Z. Huang, S. Zhang, T. B. Norris, and N. A. Kotov, *Nat. Mater.* **2019**, 18, 820-826

[21] Q. Zhang, E. Plum, J. Y. Ou, H. Pi, J. Li, K. F. MacDonald, and N. I. Zheludev, Adv. Opt. Mater. **2020**, 10.1002/adom.202001826

[22] M. Liu, Q. Xu, X. Chen, E. Plum, H. Li, X. Zhang, C. Zhang, C. Zou, J. Han, and W. Zhang, *Sci. Rep.* **2019**, 9, 4097

[23] M. Liu, E. Plum, H. Li, S. Duan, S. Li, Q. Xu, X. Zhang, C. Zhang, C. Zou, B. Jin, J. Han, and W. Zhang, *Adv. Opt. Mater.* **2020**, 8, 1901572

[24] Q. Y. Wen, H. W. Zhang, Q. H. Yang, Y. S. Xie, K. Chen, and Y. L. Liu, *Appl. Phys. Lett.* **2010**, 97, 021111

[25] T. Driscoll, S. Palit, M. M. Qazilbash, M. Brehm, F. Keilmann, B.-G. Chae, S.-J. Yun, H.-T. Kim, S. Y. Cho, N. M. Jokerst, D. R. Smith, and D. N. Basov, *Appl. Phys. Lett.* **2008**, 93, 024101

[26] H. Cai, S. Chen, C. Zou, Q. Huang, Y. Liu, X. Hu, Z. Fu, Y. Zhao, H. He, and Y. Lu, *Adv. Opt. Mater.* **2018**, 6, 1800257

[27] Y. H. Zhu, Y. Zhao, M. Holtz, Z. Y. Fan, and A. A. Bernussi, *J. Opt. Soc. Am. B* **2012**, 29, 2373-2378

[28] Y. Zhu, S. Vegesna, Y. Zhao, V. Kuryatkov, M. Holtz, Z. Fan, M. Saed, and A. A. Bernussi,

Opt. Lett. **2013**, 38, 2382-2384

[29] X. Xiong, W. H. Sun, Y. J. Bao, M. Wang, R. W. Peng, C. Sun, X. Lu, J. Shao, Z. F. Li, and N. B. Ming, *Phys. Rev. B* **2010**, 81, 075119

[30] R. K. Zhao, T. Koschny, and C. M. Soukoulis, *Opt. Express* **2010**, 18, 14553-14567

[31] Z. Li, R. Zhao, T. Koschny, M. Kafesaki, K. B. Alici, E. Colak, H. Caglayan, E. Ozbay, and C. M. Soukoulis, *Appl. Phys. Lett.* **2010**, 97, 081901

[32] Y. Zhao, M. Belkin, and A. Alu, *Nat. Comun.* **2012**, 3, 870

[33] O. L. Muskens, L. Bergamini, Y. Wang, J. M. Gaskell, N. Zabala, C. H. de Groot, D. W. Sheel, and J. Aizpurua, *Light: Sci. Appl.* **2016**, *5*, e16173

[34] M. Liu, E. Plum, H. Li, S. Li, Q. Xu, X. Zhang, C. Zhang, C. Zou, B. Jin, J. Han, and W. Zhang, University of Southampton ePrints research repository, https://doi.org/10.5258/SOTON/D1646

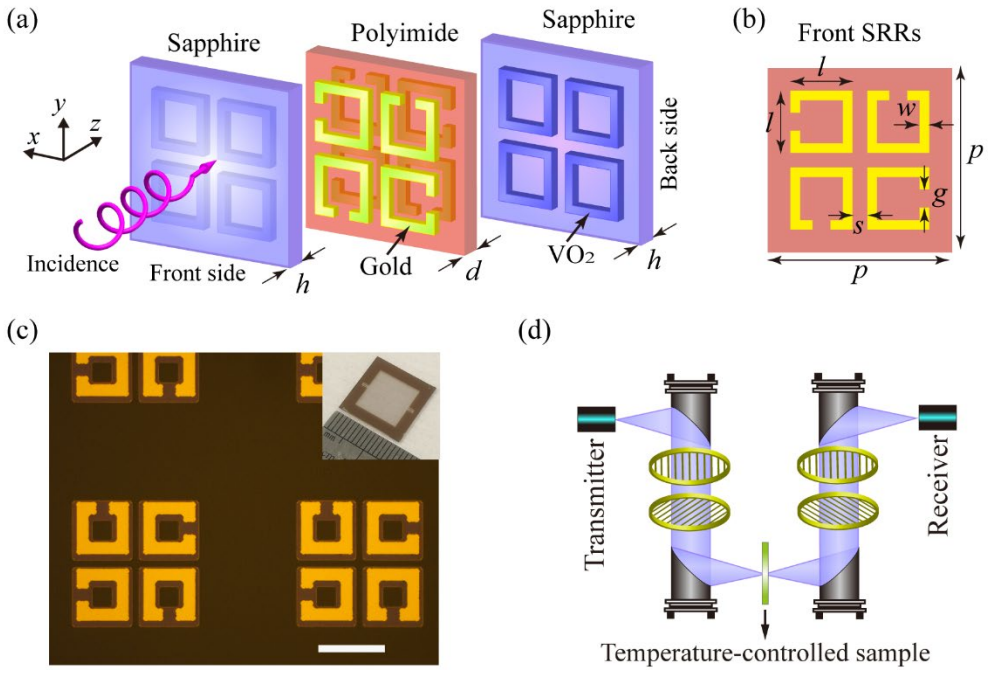

Figure 1. Metamaterial with switchable chirality. (a) Unit cell, composed of pairs of identical and mutually twisted gold SRRs in parallel planes sandwiched in between square VO_2 rings with geometrical parameters h = 1000 µm, d = 33 µm, l = 33 µm, w = 9 µm, p = 135 µm, g = 6 µm and s = 7 µm. All layers are placed directly on top of each other. (b) SRR layer of the unit cell, containing SRRs rotated in 90° steps to achieve an isotropic response. (c) Optical microscope image of gold SRRs and VO_2 square rings with a 40 µm scale bar. The inset shows a photo of the whole sample. (d) Sample characterization by THz-TDS.

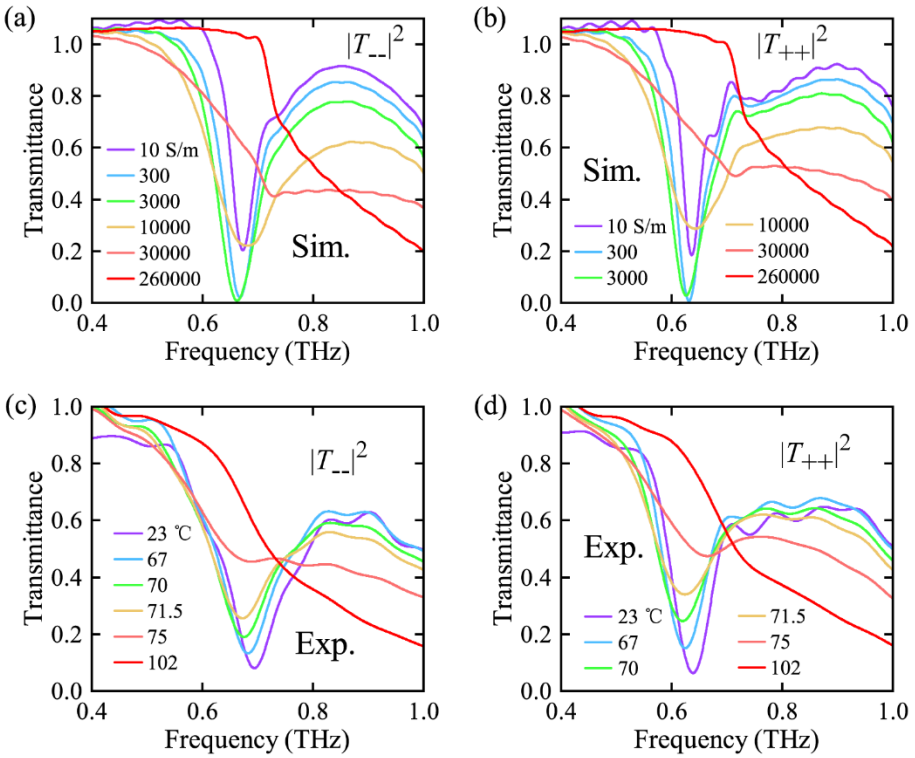

Figure 2. Switching of the transmittance for circularly polarized waves as the VO_2 phase transitions from insulating to metallic. Simulated frequency dependence of co-polarized transmittance for (a) LCP (-) and (b) RCP (+) for VO_2 conductivities ranging from 10 S/m to 2.6×10^5 S/m. Measured frequency dependence of co-polarized transmittance for (c) LCP and (d) RCP at temperatures ranging from 23 ℃ to 102 ℃. $|T_{ij}|^2$ represents the *i*-polarized transmittance of the sample resulting from *j*-polarized illumination. $|T_{-+}|^2$ and $|T_{+-}|^2$ are negligible in all cases.

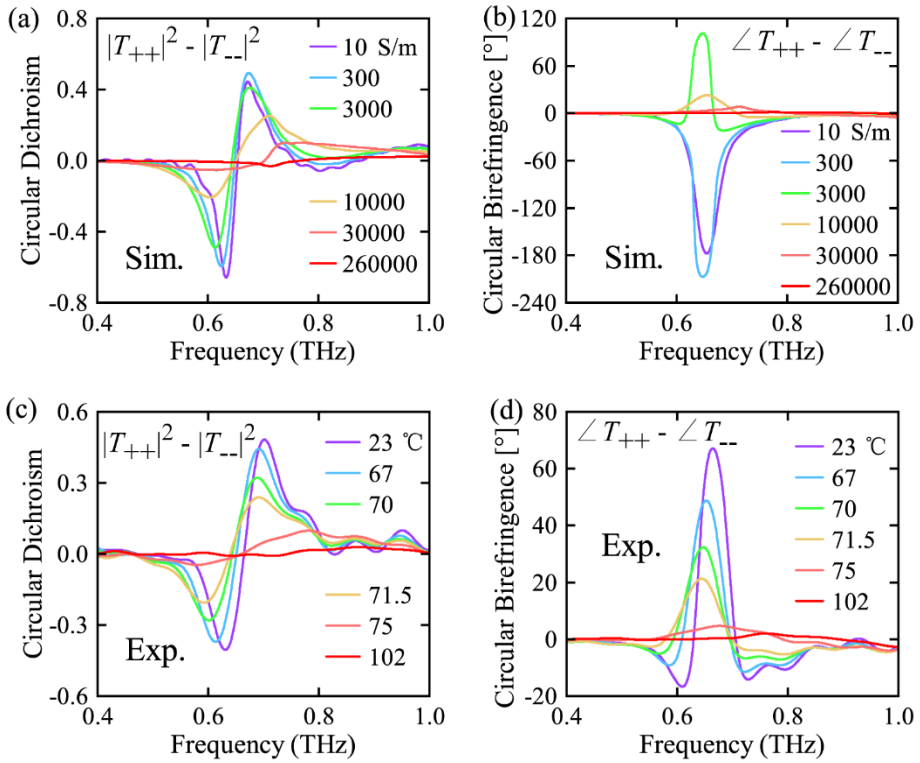

Figure 3. Switching of optical activity as VO_2 transitions from insulating to metallic. Simulated frequency dependence of (a) circular dichroism and (b) circular birefringence for VO_2 conductivities σ ranging from 10 S/m to 2.6×10^5 S/m. Measured frequency dependence of (c) circular dichroism and (d) circular birefringence at temperatures ranging from 23 ℃ to 102 ℃.

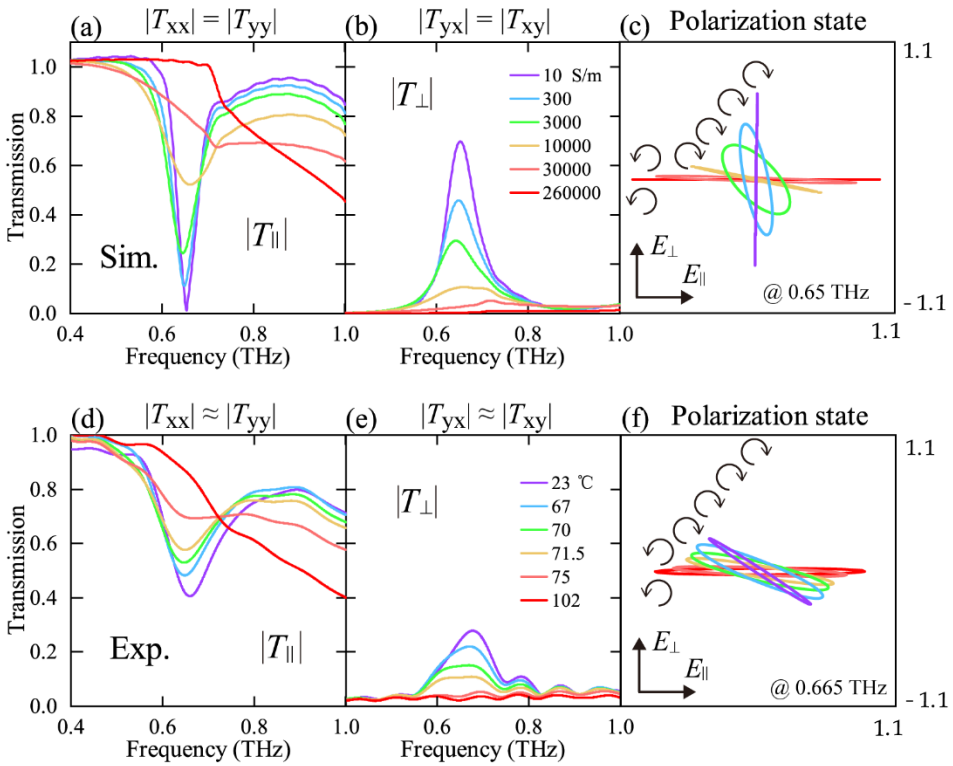

Figure 4. Switching of linear polarization conversion as VO_2 transitions from insulating to metallic. Simulated frequency dependence of (a) co- and (b) cross-polarized transmission amplitude for linearly polarized waves for VO_2 conductivities ranging from 10 S/m to 2.6×10^5 S/m. (c) Transmitted polarization state at 0.65 THz for incident linearly polarized waves. Measured frequency dependence of (d) co- and (e) cross-polarized transmission amplitude for linearly polarized waves at temperatures ranging from 23 ℃ to 102 ℃. (f) Transmitted polarization state at 0.665 THz for incident linear polarization. Polarization ellipses are shown as seen by an observer looking from the receiver at the source.

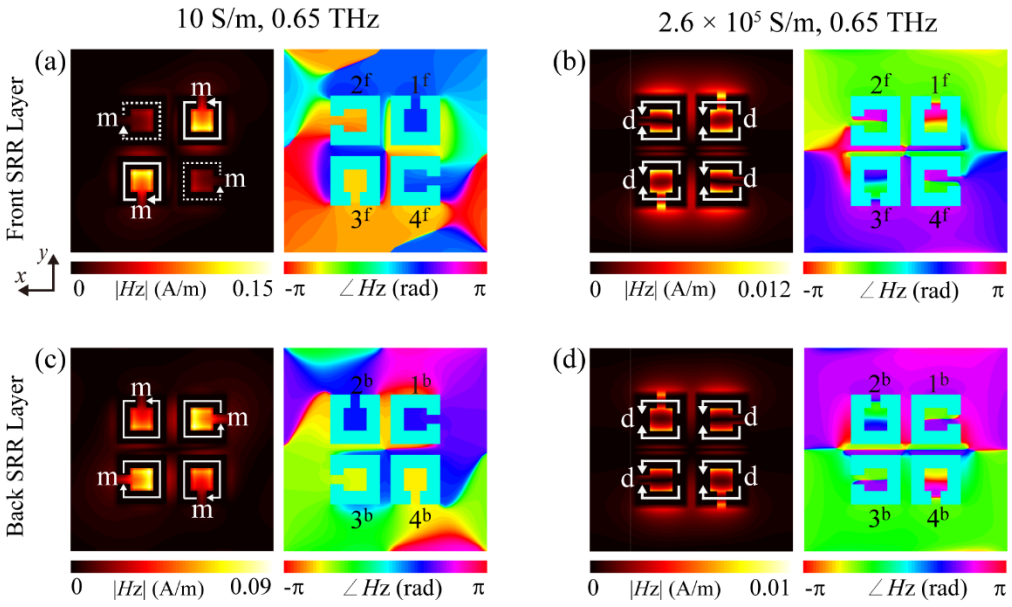

Figure 5. Physical mechanism of switchable linear polarization conversion in the hybrid 3D-chiral metamaterial. Modes excited on the (a, b) front SRRs layer and (c, d) back SRRs layer by an *x*-polarized 0.65 THz wave normally incident on the front side of the metamaterial when VO_2 is in its (a, c) insulating room-temperature phase (σ = 10 S/m) and (b, d) conductive high-temperature phase ($\sigma = 2.6 \times 10^5$ S/m). Amplitude and phase of the magnetic field H_z is shown within the SRR planes. The instantaneous directions of currents are marked by white lines with arrows. The currents correspond to magnetic and electric dipoles, **m** and **d**, for low and high VO_2 conductivity, respectively. The front and back split rings are labelled 1^f to 4^f and 1^b to 4^b, respectively.

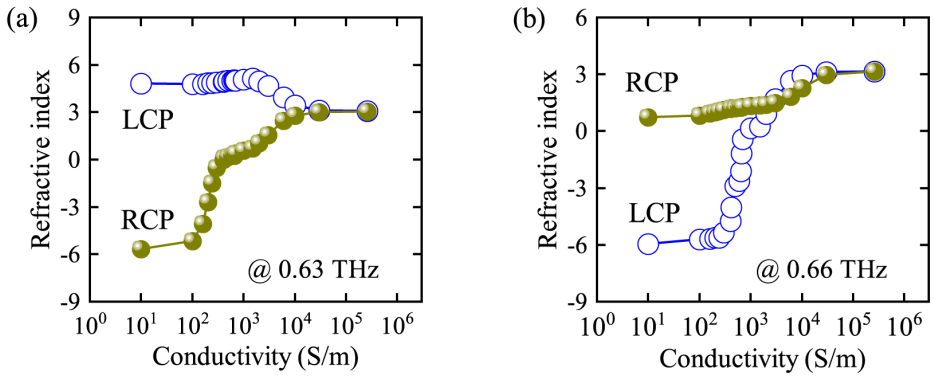

Figure 6. Refractive index for RCP and LCP waves at (a) 0.63 THz and (b) 0.66 THz as a function of VO_2 conductivity according to numerical simulations.

Table of Contents Entry

Phase transitions enable active control over the symmetry of matter. We exploit the metal-to-insulator transition of vanadium dioxide to switch an artificial material between chiral and achiral states. The metamaterial's chiral-to-achiral transition controls its electromagnetic properties, where optical activity is turned on/off and the refractive index changes between negative and positive values.

Meng Liu, Eric Plum,* Hua Li, Shaoxian Li, Quan Xu, Xueqian Zhang, Caihong Zhang, Chongwen Zou, Biaobing Jin, Jiaguang Han,* and Weili Zhang*

Temperature-controlled optical activity and negative refractive index

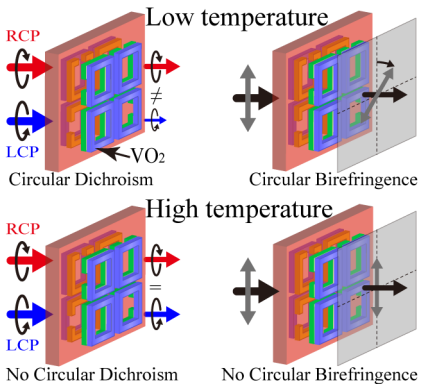

Supporting Information

Temperature-controlled optical activity and negative refractive index

Meng Liu, Eric Plum, Hua Li, Siyu Duan, Shaoxian Li, Quan Xu, Xueqian Zhang, Caihong Zhang, Chongwen Zou, Biaobing Jin, Jiaguang Han, and Weili Zhang

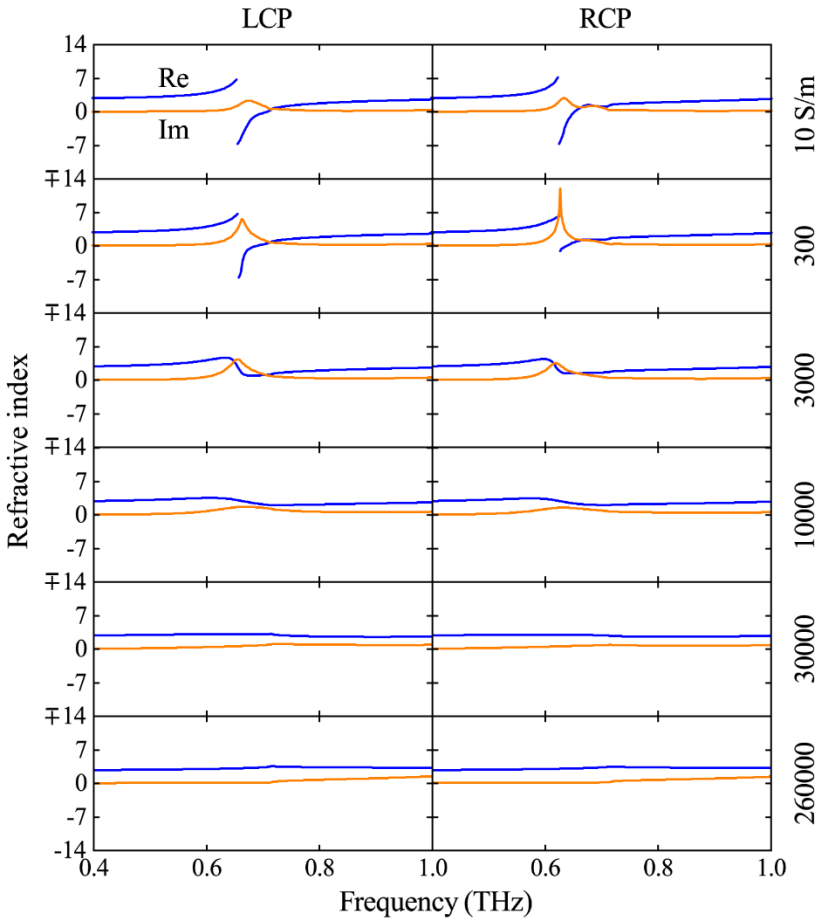

Figure S1. Refractive index for LCP (left) and RCP (right) as a function of frequency for different conductivities of VO_2 according to numerical simulations.